

Identifying causal relationships for land cover changes in Ghana using satellite remote sensing

Sirapoom Peanusaha (ASABE ID: 1057379)

s.peanusaha@gmail.com, Tel. (+1) 352-871-2200

University of Florida, Gainesville, Florida

B.S. in Biological Engineering (Anticipated Graduation: August 2020)

Under the direction of Dr. Jasmeet Judge

Department of Agricultural and Biological Engineering, University of Florida

Student Contestant: Sirapoom Peanusaha Date: 5/20/2020

Student Branch Advisor: Richard Y. Rholts Date: 5/14/2020

Origin of Research

SERVIR Program is a joint venture between the National Aeronautics and Space Administration (NASA) and the United States Agency for International Development (USAID). The program is aimed to provide remote sensing and geospatial tools to build technical capacity and create transformational changes to user-customized decision-making in developing countries. The SERVIR program stretches across three continents in five regions namely Amazonia, West Africa, East & South Africa, Himalaya, and Mekong. The thematic areas include agriculture and food safety; water resources and hydroclimatic disaster; land use and land cover change (LULCC) & ecosystems; and weather and climate.

Recently, SERVIR funded project as a part of the SERVIR-Applied Science Team for West Africa under the LULCC theme titled "*Linking deforestation, urbanization, and agricultural expansion for land-use decisions in Ghana*". The aim of the project, led by Prof Jasmeet Judge, is to provide effective land use planning framework to land managers in Ghana using satellite remote sensing and GIS-based analysis tools to meliorate land use planning in Ghana. The project team consists of research experts from the University of Florida, and the Center for Remote Sensing and GIS (CERSGIS), Ghana; technical partners from the Land Use and Spatial Planning Authority (LUSPA); and the end-user at the District Assemblies (DA). This research project is conducted as a precursor to developing a methodology for quantifying remote sensing-based causal linkages among various natural and anthropogenic factors in LULCC that will be used to inform the land use planning framework.

Acknowledgements

I would like to acknowledge the NASA-USAID SERVIR program (Award # 80NSSC20K0153) and the UF Agricultural and Biological Engineering Department Undergraduate Research Award for their funding to pursue this research project. I would like to thank Prof. Aditya Singh for providing insights on data sets retrieval and interpretation, Prof. Rachata Muneeppeerakul for providing insights on the causal linkages, and George Worrall for teaching me Python and other statistical tools. Lastly, I would like to express my gratitude to Prof. Jasmeet Judge for providing me endless opportunities to learn and improve myself, and for supervising this research project.

Abstract

Effective natural resource management, conservation of biodiversity, and sustainable land use plan required understanding of the drivers and the causes of the land cover change (LCC). The tropical regions around the world have experienced tremendous LCC over the past decades. Complex interactions among humans, climate, and land pose challenges to the attainment of such understanding. Satellite remote sensing provides time series data that could be utilized to understand these complex interactions. The advantage of satellite remote sensing is its availability in data-poor regions such as in developing countries. Nonetheless, remote sensing-based methods to identify and quantify precursors to LCC are still in their infancy. This research project explored a recently developed methodology which utilized remote sensing data to understand the causal relationships in the interaction between LCC and underlying natural conditions. The method used four remote sensing-based factors, namely evapotranspiration (ET), albedo (α), surface temperature (T_s), and normalized difference vegetation index (NDVI). In this study, this methodology was implemented from 2001-2016 in four districts in Ghana with varying LCCs to assess the extendibility and potential to provide insight into the precursors of LCC. The annual median of the four RS-based factors was used to obtain correlations and causal relationships in these Districts. The result suggested that the methodology was highly sensitive to how remote sensing data were analyzed and need to be further improved with new structural formulations to increase its robustness. In addition, anthropogenic factors such as illegal mining and logging need to be incorporated to provide realistic linkages in the region.

Keywords: land cover change (LCC), satellite remote sensing, causal relationship, Ghana, West Africa

Introduction

Understanding drivers and causes of land cover changes (LCC) in various biomes is critical for effective management of natural resources, conservation of biodiversity, and development of sustainable land use plans. Tropical regions around the world have experienced tremendous LCC, with intense deforestation in the past decades (Lewis, Edwards, & Galbraith, 2015). For example, in West Africa, about 30 percent of the Upper Guinean Forest (UGF) has been disrupted since 1975 (CLISS, 2016). The remaining 18 percent of the UGF is located in Ghana and it accounts for about 24 percent of the country's land coverage. Even though the deforestation rates have slowed in recent year, Ghana still experiences significant anthropogenic pressures causing human-driven land use change. The major drivers of deforestation include logging; firewood extraction; wildfire; mining; agricultural expansion for the major cash crop such as cocoa and pineapple plantations; rapid urbanization; and migration from rural areas (Addo-Fordjour & Ankomah, 2017; Appiah et al., 2009; Damnyag et al., 2013; Kusimi, 2008; Tutu Benefoh et al., 2018). Additionally, the deforestation is further intensified by poverty, by demand for agricultural and forestry product for markets overseas (Alo & Pontius, 2008; Edusah, 2011; Kusimi, 2008), and by the inadequate infrastructure and enforcement mechanisms (Aha & Ayitey, 2017; Nang, 2016; Schoneveld & German, 2014).

Satellite remote sensing provides time series of global observations that can be used to understand these complex linkages. These are particularly useful for LCC studies in data-poor regions such as developing countries. Remote Sensing (RS) of different wavelengths, such as optical; infrared; and microwave, provide complementary information regarding the land surface. For example, Lambin & Ehrlich (1997), used the Global Area Coverage (GAC) radiances measured from the Advance Very-High Resolution Radiometer (AVHRR) on the National Oceanic and Atmospheric Administration's orbiting platforms to map the land cover (LC) and LCC of the Africa continent and created LCC map from 1982 to 1991. Yuan et. al. (2005) developed a methodology to map LCC using the multitemporal Landsat Thematic Mapper (TM) data. However, many studies that use RS data to understand LCC have mainly

used correlations to interpret the relationships among key factors. For example, Vanacker et. al. (2005) mapped the LCC of sub-Saharan Africa, identified the correlation between the fluctuation in rainfall and the interannual LCC, and found that the magnitude of LCC in sub-Saharan Africa region was significantly related to rainfall variability at the 5% level and that regions with uniform herbaceous vegetation showed the highest sensitivity to rainfall fluctuation. Li et. al. (2015) used the correlation between surface temperature (T_s) and evapotranspiration (ET) to study the dynamics of the hydro-heat feedback loop and found the turning point when the ecological restoration efforts in Qinghai, China started showing positive effects by increasing the ET and resulted in grassland expansion. A significant methodological gap still remains to link the LCC and its cause since correlations do not imply causation. Some studies identified drivers of LCC through qualitative methods. For example, Kleemann et al. (2017) assessed the driving force of the LCC in northeastern Ghana using spatial analysis and experts' interviews. The major driving force identified, such as population growth in rural areas, is very informative towards understanding the precursor to LCC. However, a major drawback of such qualitative method is that the relationship between the cause and its effect is not quantifiable. Identifying and quantifying causal linkages using RS for LCC is still an active area of research.

Recently, Li et. al. (2019) developed comprehensive indicator (CI) from the residual of Pearson's correlation coefficient of four, RS-based and field-based, key natural indicators, such as evapotranspiration (ET), albedo (α), surface temperature (T_s), and normalized difference vegetation index (NDVI), to identify direct-indirect causation, and association among these indicators. The study identified the spatial correlations and temporal synchronicity among the key indicators and identified the CIs of three grassland ecosystems in China. The results confirmed the feedback mechanisms described in the theories of eco-climatology and that the temporal lag effects of ecological succession found among the three ecosystems reflects the causalities, which were described by CIs, among the key indicators. This result suggested a possibility to use CI to identify the precursors of LCC based on the causalities among the driving forces of LCC previously explored by other studies.

The goal of this study is to understand the applicability of the RS-based CI methodology in identifying causal linkages in tropical regions such as Ghana. The objective of this study is to, 1) identify the correlation between ET, α , Ts, and NDVI in the past 15 years, 2) to identify the causal linkages by finding CI for the last 15 years, and 3) to understand the relationship between the change in the key ecological structure indicators and the LCC occurred within the region.

Study Regions and Data Sets

Study Regions

The study was conducted on four distinct areas (Figure 1) in Western, Central, Eastern and Northern region of Ghana representing different LCC trend from 2001 to 2016: (1) Tarkwa Nsuem municipal in Wassa West District in the Western Region, (2) Tamale metropolitan in the Northern Region, (3) Atiwa district in the Eastern Region and, (4) Twifo-Hemang Lower Denkyira District (THLDD) in the Central region.

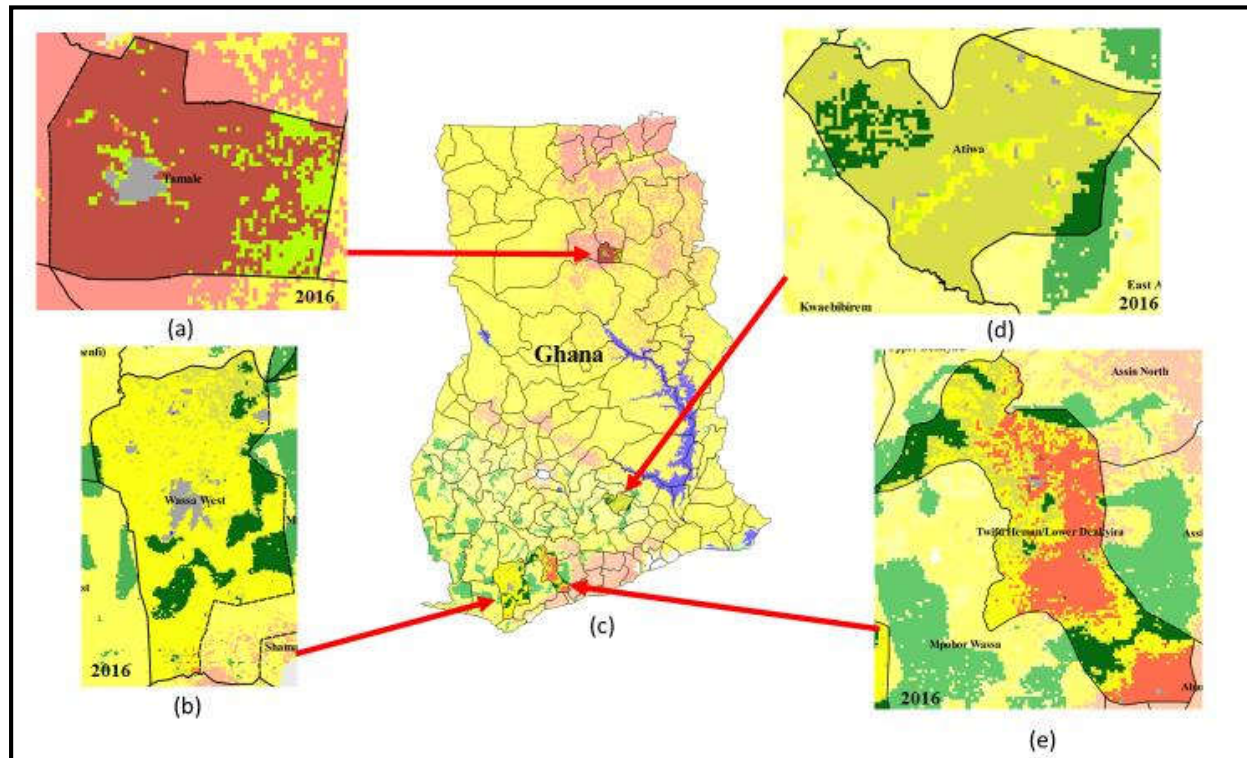


Figure 1 Study Regions used in the study (a) Land Cover map of Tamale in 2016 (b) Land Cover map of Tarkwa in 2016 (c) Land Cover map of Ghana with the study regions highlighted (d) Land Cover map of Atiwa District (e) Land Cover map of Twifo-Hemang Lower Denkyira District (THLDD). The figure is displayed in International Geosphere-Biosphere Program (IGBP) color scheme.

In Tarkwa, deforestation for mining was widespread and the unmined areas represented the farmland (Schueler, Kuemmerle, & Schröder, 2011). Tarkwa was selected as one of the study regions due to its significant LCC from forest to mining, agriculture, and urban area. Tarkwa experienced the most drastic LCC in all the study regions (Figure 2b). In 2001, more than half of the region is covered with either Evergreen needleleaf forest or Woody savannas. The region experience reduction in both forest and cropland while experienced significant urban growth. The agricultural land was replaced by surface gold mining (Schueler et al., 2011) which was represented as savannas in the IGBP LC map. Tarkwa was selected to represent the area that experienced drastic LCC with both urban and agricultural expansion. Tamale Metropolitan area is the capital city of the Northern region of Ghana. Tamale Metropolitan area covers about 647 km² and had about 275,000 population in 2019. Tamale is the third largest and the fastest growing city in Ghana (Kuusaana & Eledi, 2015). The LC type in Tamale remained more than 90

percent of agriculture from 2001 to 2016 (Figure 2c). Tamale has the highest percentage in terms of urbanized population per total population in Ghana and is located in the Guinea savannah zone far away from the coastline which provides a sample for in a drier climate zone with as compared to Tarkwa, and THLDD which are located near the coastline. Tamale was selected to represent the area with static LCC where the majority of LC is a combination of croplands and open grassland. Atiwa district had area cover about 1,166 km² and had the about 137,000 population in 2019. Atiwa comprised of a hilly region and the climate conditions is ideal for growing food crops such as maize and yam. The district experienced a slight increase in forest area and a slight decrease in agricultural land (Figure 2d). The LCC in Atiwa is very recognizable in the way that the woody savannah areas along the southwest-northeast corridor were replaced by savannah which suggested that the forest was cut down along the transportation route. Moreover, there were small clusters of urban areas that expanded along the transportation route. Atiwa was selected to represent the area that has a steady LC with the forest being the dominant LC which in turn made Atiwa the area with the least human-driven LCC among all four study regions. Lastly, Twifo-Hemang Lower Denkyira District (THLDD) is located in the Central region and had a population of about 170,000 in 2010. About a quarter of the district consists of forest reserves which include the Kakum National Park. THLDD experienced a very clear pattern of agricultural expansion and deforestation. The forest areas on the eastern side of the district were replaced by cropland and savannah. The woody savannah in the central-eastern side of the district was also replaced by savannah which indicated deforestation. The climate in the district is ideal for cocoa, palm oil, and other cash crop plantation. THLDD was selected to represent with mixed LC with about 50 percent forest and 50 percent agriculture in 2016 (Figure 2e).

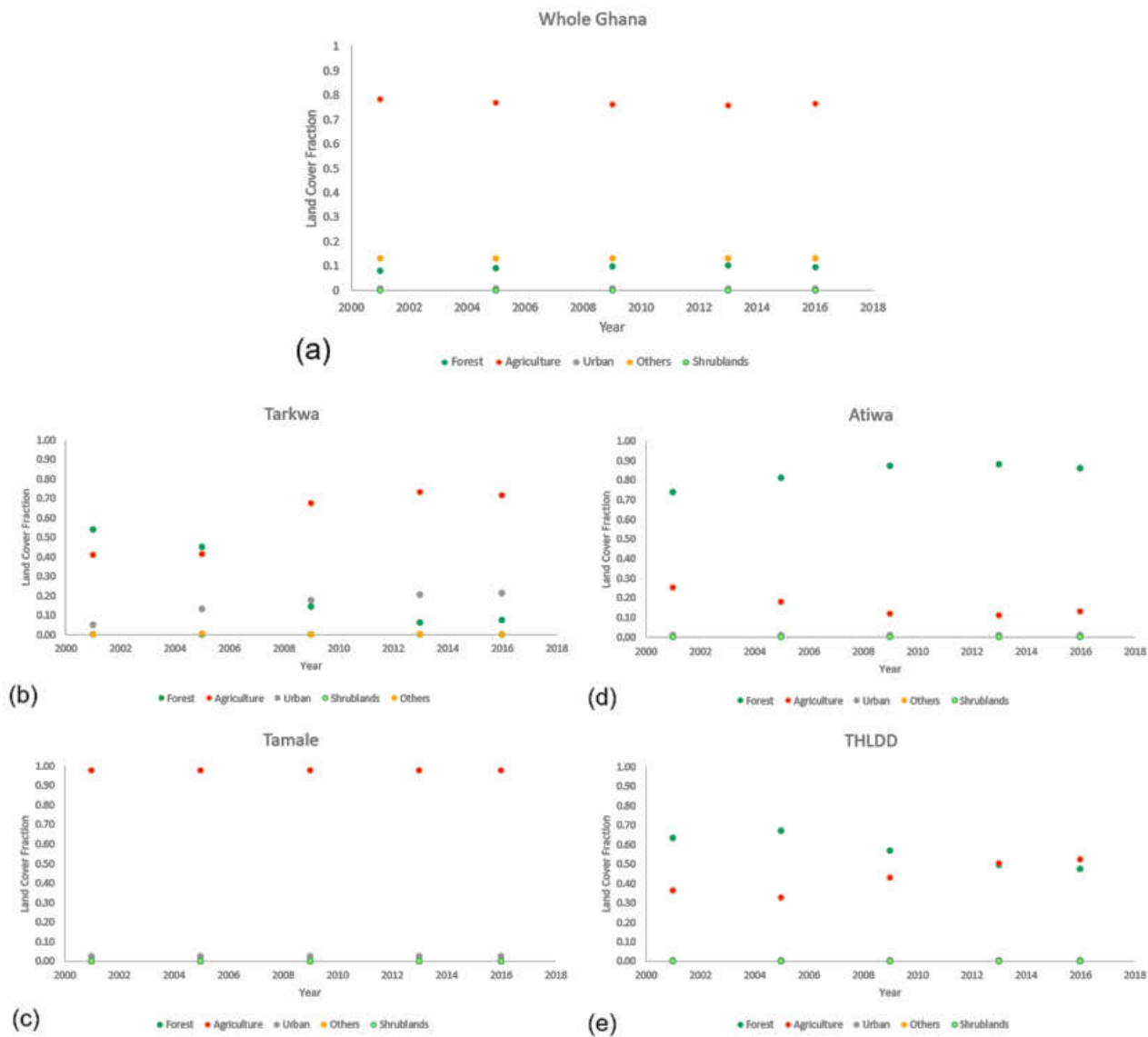


Figure 2 Land cover fraction of the study regions (a) Land cover fraction of whole Ghana (b) Land cover fraction of Tarkwa (c) Land cover fraction of Tamale (d) Land cover fraction of Atiwa (e) Land cover fraction of THLDD

Data Sets

Table 1 represents the data sets used in the study. In order to format the data with different temporal resolutions to have the same temporal length, the data of the four key indicators, namely α , NDVI, T_s , and ET, were compiled on a yearly basis and the temporal median value represented the specific indicator of each year. The data sets were obtained from *Google Earth Engine* (GEE) via *Javascript*. For each set of indicator data, the low-quality pixels that contained distorted values were filtered out during the data compilation process on GEE by using the *QA bitmasking* process. The LC data sets, provided on an annual basis, were downloaded in the International Geosphere-Biosphere Program (IGBP) LC classification. The IGBP LC scheme is divided into 17 categories ranging from Evergreen Needleleaf Forest to Water Bodies.

Table 1 The data sets used in the study

Data and products	Source	Temporal Resolution [days]	Spatial Resolution [m]
Land cover (LC)	NASA MODIS	365	500
Albedo (α)	NASA MODIS	1	500
Normalized Difference Vegetation Index (NDVI)	NASA MODIS	16	500
Surface temperature (T_s)	NASA MODIS	1	1000
Evapotranspiration (ET)	NASA MODIS	8	500

In this study, the 17 categories were simplified into five categories: forest, shrublands, agriculture, urban, and others. The Evergreen Needleleaf Forests, Evergreen Broadleaf Forests, Deciduous Needleleaf Forests, Deciduous Broadleaf Forests, Mixed Forests, and Woody Savannas were reclassified to be the Forests. The Closed Shrublands and the Open Shrublands were reclassified as the Shrublands. The Urban and Built-up Lands were reclassified as Urban. The Savannas, Grasslands,

Croplands, and Cropland/Natural Vegetation Mosaics were reclassified as the Agricultural Lands. The Permanent Wetlands, Permanent Snow and Ice, Barren, Water Bodies were reclassified as the Others. All the data sets mentioned were downloaded in the .tiff file format. There were two time-intervals used in this study: every 2 years and every 4 years. The 2-year interval consisted of data sets from the year 2001, 2003, 2005, 2007, 2009, 2011, 2013, and 2016. The 4-year interval consisted of data sets from the year 2001 2005, 2009, 2013, and 2016. The study only included the data set until 2016 because the MODIS NDVI data set on GEE was available up until March 6, 2017.

Methodology

Identifying the correlations among the key indicators

Three pairs of key indicators, namely NDVI- α ; α -T_s; and T_s-ET, were selected on the as representations of the cause-effect vegetation and regional climate processes (Li et al., 2015). In this study, the correlations were used to compare to those obtained in China from the original implementation. The correlations were conducted on data at the 4-year interval. The correlations of NDVI- α , α -T_s, and T_s-ET were calculated for each year separately. The correlation of each pair were lined up as a time series data set and compared across four study regions and the whole Ghana.

Identifying the LCC trend

The LCC trend was processed using *Python3* and *Jupyter Notebook*. LC raster files were imported into the *Jupyter Notebook* workspace and clipped by the *gdal.Translate* command to convert the raster that covers the whole Ghana area to the study regions via the rectangular box raster extraction method. The raster data was flattened from 2-D data set to a 1-D array. Any individual pixel with at least 'Nan' value was filtered out from all the raster data to create a complete set of data with no null value. The sum of each type of simplified LC scheme was calculated. Finally, the sum of each LC type was divided by the total number of pixels to calculate the LC type fractions for each year. The LCC was calculated based on the raster data of the 4-year interval (Figure 2 a-d). The LC fraction calculation was

performed on Whole Ghana, Tarkwa Nsuem municipal, Tamale metropolitan area, Atiwa District, and THLDD.

Calculating the CI

The CI equation can be explained as the following:

$$C(X,Y) = \frac{\left(\left| P\left(X, \frac{dY}{dt}\right) \right| + \left| P\left(\frac{dX}{dt}, \frac{d^2Y}{dt^2}\right) \right| \right) - \left(\left| P\left(X, \frac{d^2Y}{dt^2}\right) \right| \right)}{\left(\left| P(X,Y) \right| + \left| P\left(\frac{dX}{dt}, \frac{dY}{dt}\right) \right| + \left| P\left(\frac{d^2X}{dt^2}, \frac{d^2Y}{dt^2}\right) \right| \right)} \quad (1)$$

where

$C(X,Y)$ = CI of the causal effect of X upon Y

$P(X,Y)$ = Pearson's correlation coefficient of X and Y

X = the time series of the spatial mean data of the cause indicator

Y = the time series of the spatial mean data of the affected indicator

t = time

$\frac{dX}{dt}$ = the first derivative of the curve fitting polynomial equation of X

$\frac{dY}{dt}$ = the first derivative of the curve fitting polynomial equation of Y

$\frac{d^2X}{dt^2}$ = the second derivative of the curve fitting polynomial equation of X

$\frac{d^2Y}{dt^2}$ = the second derivative of the curve fitting polynomial equation of Y

Figure 3 represents the flow diagram of calculating the CI, where $C(X,Y)$ represents the CI between indicator X, the cause, and indicator Y, the affected variable. The CI calculation was performed using *Python3* and *Jupyter Notebook*. A set of raster data that contained the yearly temporal median of the α , NDVI, T_s , and ET were imported into the workspace. The raster was clipped by the *gdal* function. The data in each pixel of the raster was imported as an array and was flattened from 2D to 1D. The value extracted was multiplied by its scale provided by the data source to reshape the value to its actual value. For example, NDVI was multiplied by a scale of 0.001 to convert its raw into the actual NDVI. In this study, there were two temporal intervals used in calculating the CI: (1) 2-years interval, and (2) 4-year

interval. Li et al. Li et al. (2019) performed the calculation using the data set that was 3-7 years apart. The goal of using two different time intervals in this study is to: (1) to observe the effect of the different time intervals on the value of a CI calculated. (2) to understand the causal relationship among the climate indicators in both short-term effects and long-term effects. The two years interval was aimed to provide insight on the causal relationship of the short-term effect and the four years interval was planned to indicate the causal relationship with long-term effect.

The data sets of the four key indicators were compiled using the *pandas* library before eliminating the pixels that have at least one 'NaN' data. Each study region had a different size. Therefore, the difference in raster size must be eliminated to prevent the raster from affecting the CI calculated. The region with the smallest raster size was Tarkwa which had a size of 1488 pixels and cover the total area of about 372 km². After eliminating the 'NaN' pixels, the Tarkwa study region had about 554 pixels left. The largest study region was THLDD which had a size of 12508 pixels. After eliminating the 'NaN' pixels, THLDD had about 9322 pixels left. Therefore, for Tamale metropolitan area, Atiwa District, and THLDD study region, 554 random sample pixels were selected to represent the whole study region. For each pair of climate indicators, the calculation was run three times and the average CIs were calculated to reduce the variation due to the randomness of the sample. The flow chart of the calculation process can be found in Figure 3.

The CIs between ET and NDVI and ET and α were excluded from the calculation because MODIS ET data set used NDVI and α both indirectly and directly as inputs to calculate ET (Figure 2, Mu, Zhao, & Running, 2013). Calculation CIs of among the three pairs of indicators would be redundant and produce inaccurate results.

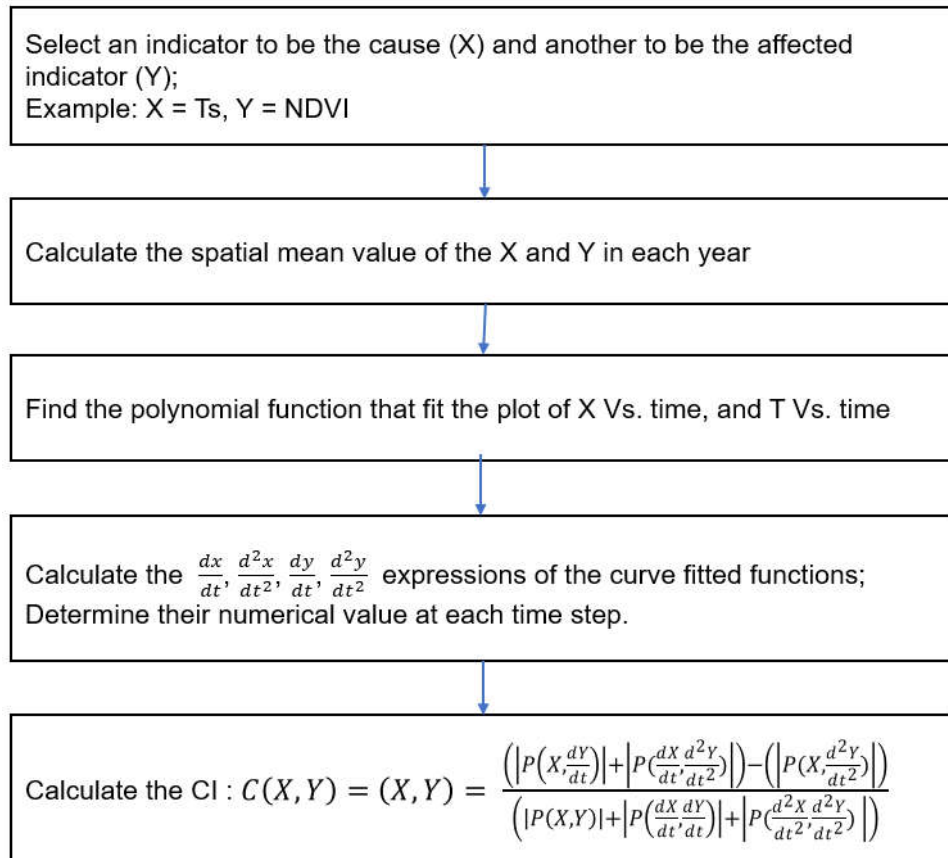


Figure 3 Flow chart diagram of the CI calculation method. The time series data sets were inputted at the first process of the flow chart

Results and Discussion

Table 2 shows the correlation between NDVI- α ; α -Ts; and Ts-ET for Ghana and the four Districts. Correlation trends of Whole Ghana all followed a similar trend found in Li et. al (2019). For whole Ghana, the correlation of NDVI- α was negative because the vegetation, which is represented by NDVI, absorbs the solar radiation, thus decrease the radiation reflected. The correlation between α -Ts was positive because the vegetated area, which had relatively high NDVI and entails low α , retain more moisture on the surface, therefore, decrease the Ts. The correlation between Ts-ET was negative because both evaporation and plant transpiration had a cooling effect on the surface. However, the correlation trends for Districts deviate from the general trend found in whole Ghana. The only region that still followed the same trend was Tamale. Tamale and Ghana both had homogenous LC type. Throughout the

15 years, Tamale LC was always about 90 percent while the Ghana LC was stable at about 80 percent (Figure 2a,2c). The heterogeneous LC type of other three districts caused the correlations to diverge because the diverse LC phenology complicated the relationship of the indicators

Table 2 Correlations of the key indicators

Area	Indicators Pair	2001	2005	2009	2013	2016
Whole Ghana	NDVI- α	-0.867	-0.876	-0.869	-0.847	-0.875
	α -T _s	0.801	0.843	0.843	0.760	0.819
	T _s -ET	-0.873	-0.890	-0.878	-0.877	-0.852
Tarkwa	NDVI- α	-0.321	-0.558	-0.746	-0.760	-0.676
	α -T _s	0.312	0.311	0.521	0.481	0.177
	T _s -ET	0.087	-0.081	-0.301	-0.188	-0.108
Tamale	NDVI- α	-0.454	-0.435	-0.609	-0.706	-0.527
	α -T _s	0.352	0.469	0.256	0.225	0.094
	T _s -ET	-0.217	-0.302	-0.065	-0.192	-0.013
Atiwa District	NDVI- α	-0.316	-0.105	0.061	-0.414	-0.268
	α -T _s	0.695	0.233	0.503	0.668	0.628
	T _s -ET	0.084	0.187	0.116	0.053	0.211
THLDD	NDVI- α	-0.047	-0.134	-0.084	-0.246	-0.202
	α -T _s	0.394	0.248	0.511	0.600	0.513
	T _s -ET	0.338	0.311	0.274	0.331	0.290

Table 3 shows the first two highest CIs in all four districts and each temporal interval and polynomial degree. The positive value of CIs shows that cause indicator, X, had a more direct effect on the affected indicator, Y (Li et al., 2019). For all four districts, the absolute highest CIs were all in positive which implied that the most prominent causal relationship found in this study is a direct causal relation. The value of the highest CIs in each category varied from the lowest at about 0.202 for the CI between α and NDVI in THLDD to the highest at about 1.433 for the CI between T_s and ET in Atiwa district. For 4 years interval, the CIs in the Atiwa District showed the strongest causal relationship among all four selected study regions. This could be because that high portion of the LC in Atiwa district is

forest and thus the causal relationship was more pronounced because there was relatively less human interference in the ecosystem. In Atiwa for 4th-degree polynomial curve fitting equation, the indicator that was found to be the major cause of change of other indicators with the top two highest CIs was NDVI which reflects the vegetation in the region. This could imply that the vegetation in the area with relatively low human interference plays a major role in shaping the LCC trend and, thus, could be utilized to predict the LCC.

Tarkwa Nsuem municipal and THLDD both showed relatively low CIs which imply low causal relationships among the indicators or that the direct and indirect causal relationship was about the same. Both regions experienced substantial LCC which was mainly driven by humans such as agricultural expansion. The low CIs implied loose causal relationships among the indicators. There is a possibility that there could be anthropogenic indicators that can be incorporated into the calculation and would result in higher CI. Such anthropogenic indicators could be the LCC driving force found in previous studies such as population growth (Kleemann, Baysal, Bulley, & Fürst, 2017).

On the other hand, Tamale CIs were relatively moderate compared to the other three study regions. The unique trend of CI pattern found in Tamale was that Ts was involved as either the cause or the affected indicators in 7 out of 8 indicators pair with the highest causal relationship (Table 3). The location and ecosystem of Tamale is unique compared to the other three regions because Tamale is the furthest location from the coastline and is in the Guinea Savannah ecological zone. Tamale comprised mainly of croplands, represented by red-colored cells, and grasslands, represented by green-colored cells, (Figure 1a) and the climate is significantly drier than the southern regions of Ghana due to its proximity to the Sahara Desert. The result could imply that the surface temperature in Tamale is more prone to change compared other that of the other regions because there is no natural stabilizer.

Table 3 The 2 highest CIs in each time interval and polynomial degree

Area	Polynomial degree	3rd degree polynomial		4th degree polynomial	
		(X,Y)	C(X,Y)	(X,Y)	C(X,Y)
Tarkwa Nsuem municipal	2 years interval	Ts- α	0.535	α -Ts	0.267
		α -Ts	0.501	α -NDVI	0.248
	4 years interval	NDVI-Ts	0.969	Ts-NDVI	0.282
		NDVI- α	0.566	α -Ts	0.253
Tamale metropolitan	2 years interval	ET-Ts	0.553	Ts- α	0.930
		NDVI- α	0.475	Ts-NDVI	0.865
	4 years interval	α -Ts	1.005	Ts-NDVI	0.437
		NDVI-Ts	0.812	Ts-ET	0.426
Atiwa District	2 years interval	Ts-NDVI	0.688	NDVI- α	0.528
		Ts- α	0.597	NDVI-Ts	0.504
	4 years interval	Ts-ET	0.749	NDVI- α	1.433
		ET-Ts	0.664	NDVI-Ts	1.285
Twifo-Hemang Lower Denkyira District	2 years interval	Ts-ET	0.305	ET-Ts	0.218
		α -NDVI	0.294	α -Ts	0.202
	4 years interval	α -NDVI	0.836	NDVI- α	0.597
		ET-Ts	0.608	NDVI-Ts	0.487

Overall CIs among indicators

The CIs set for the 4 years interval with 4th-degree polynomial showed the highest overall CIs set. Figure 4 represents all the CIs pair in the given interval and polynomial for all study regions. The set of CIs besides that of Atiwa shows no significant causal relationship (Figure 4a, 4b, 4d). The other similar trend found between the CIs in the previous study by Li et. al. (2019) and in this study was that Tamale which has a climate similar to arid grassland in China shares the trend of having Ts as the indicator with high CIs value. For Atiwa and THLDD, NDVI was the indicator that had the highest CIs. In contrast, two of three studied areas in China showed a very high causal relationship between NDVI-ET, ET-NDVI, and α -ET which were excluded from the calculation as described in the methodology section. Moreover, the CI found in the previous study were much stronger: the highest CI found were in the margin between 3.5 and 4.3 while the highest CIs found in this study were 1.433.

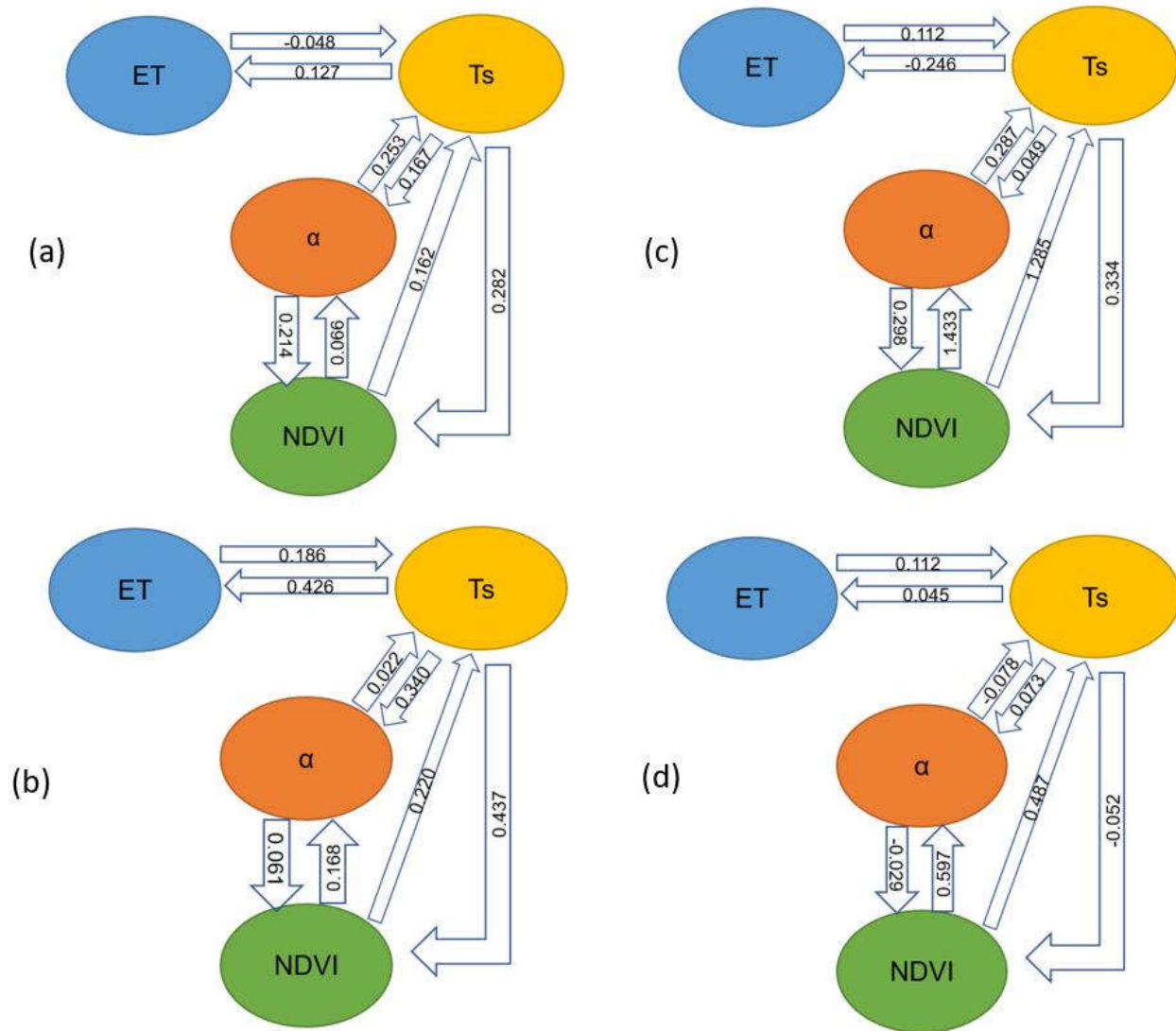


Figure 4 Overall Cis for 4 years interval with 4th degree polynomial equation (a) CIs of Tarkwa (b) CIs of Tamale (c) CIs of Atiwa District (d) CIs of Twifo-Hemang Lower Denkyira District (THLDD). The number in the arrows represent the $C(X,Y)$. The indicator at the base of the arrow was the cause (X) and the indicator that the arrow pointed towards was the affected indicator (Y).

Methodology sensitivity to polynomial degree

The major applicability issue that the preexisting CI has is that the polynomial degree did have a significant effect on the CI calculated. Once the degree of the polynomial function used to fit the curve changed, both the indicator pairs with the top two highest values and the CIs themselves changed

drastically (Table 3). The variability could pose challenges if this methodology was to be utilized to understand the precursor to LCC.

Methodology sensitivity to different time interval

The second variability found in the current method is that the CI depended on the temporal interval of data sets. The change in temporal interval caused both the highest CIs and their indicator pairs to change completely in some cases (Table 3). Although, it was anticipated that the 2 years interval would represent the causal relationships that have a short-term causal relationship while the 4 years interval was supposed to represent that of the long-term. An extensive understanding of the effect that temporal interval has on the CI must be obtained to formulate a rigid criterion to determine the appropriate temporal interval to be utilized. Additionally, the use of annual median data to represent the annual data set could undermine the seasonal change, especially for NDVI which varies throughout the growing season of the crop.

Future development of CI methodology

Method of identification and quantification of causal linkages using RS are still in their infancy. The current CI methodology still shows variability and uncertainty in terms of the accuracy of causal relationship prediction. In this study, no anthropogenic factors were included in the calculation. The results from correlation and CIs comparison suggested that the type of ecosystems and geographical characteristics affected the trend in CI. For further development of the current CI methodology, the following steps should be taken to improve the understanding of the result and the accuracy of the methodology: (1) structural equation improvements so that the method is able to use seasonal data, which is particularly important in agricultural regions; (2) incorporate anthropogenic factors into the analysis to provide realistic linkages; (3) implement methodology to more study regions with a diverse set of ecosystem types and geographical characteristics. The latter will improve the understanding of the

specific trend in CI that might occur in a specific ecosystem or geographical characteristic and will ensure more applicability of the methodology across diverse locations.

Conclusion

In this study, the newly developed methodology which utilized RS data to understand causal relationships was implemented in four districts in Ghana to test its applicability and its potential to provide insight into the precursor of LCC. The result of the study showed that LC patterns have a significant impact on the CI. More importantly, the study also revealed possible methodological flaws that the current CI method is sensitive to the temporal interval and to different polynomial degree curve fitting. Further studies could be developed to gain an understanding of how different ecosystems could lead to different trends of CIs. However, in terms of developing a reliable methodology to identify and quantify the precursor to LCC, the methodology explored in this study requires significant improvement. Future scope of the study includes the incorporation of anthropogenic factors, structural equation improvement, and implementation of the methodology to a diverse set of ecosystems.

References

- Addo-Fordjour, P., & Ankomah, F. (2017). Patterns and drivers of forest land cover changes in tropical semi-deciduous forests in Ghana. *Journal of Land Use Science*, *12*(1), 71–86. <https://doi.org/10.1080/1747423X.2016.1241313>
- Aha, B., & Ayitey, J. Z. (2017). Biofuels and the hazards of land grabbing: Tenure (in)security and indigenous farmers' investment decisions in Ghana. *Land Use Policy*, *60*, 48–59. <https://doi.org/10.1016/j.landusepol.2016.10.012>
- Alo, C. A., & Pontius, R. G. (2008). Identifying systematic land-cover transitions using remote sensing and GIS: The fate of forests inside and outside protected areas of Southwestern Ghana. *Environment and Planning B: Planning and Design*, *35*(2), 280–295. <https://doi.org/10.1068/b32091>
- Appiah, M., Blay, D., Damnyag, L., Dwomoh, F. K., Pappinen, A., & Luukkanen, O. (2009). Dependence on forest resources and tropical deforestation in Ghana. *Environment, Development and Sustainability*, *11*(3), 471–487. <https://doi.org/10.1007/s10668-007-9125-0>
- CLISS. *Landscapes of West Africa: a Window on a Changing World*. Garreston: U.S. Geological Survey, 2016.
- Damnyag, L., Saastamoinen, O., Blay, D., Dwomoh, F. K., Anglaaere, L. C. N., & Pappinen, A. (2013). Sustaining protected areas: Identifying and controlling deforestation and forest degradation drivers in the Ankasa Conservation Area, Ghana. *Biological Conservation*, *165*, 86–94. <https://doi.org/10.1016/j.biocon.2013.05.024>
- Edusah, S. (2011). The impact of forest reserves on livelihoods of fringe communities in Ghana. *Journal of Science and Technology (Ghana)*, *31*(1). <https://doi.org/10.4314/just.v31i1.64882>
- Kleemann, J., Baysal, G., Bulley, H. N. N., & Fürst, C. (2017). Assessing driving forces of land use and land cover change by a mixed-method approach in north-eastern Ghana, West Africa. *Journal of Environmental Management*, *196*, 411–442. <https://doi.org/10.1016/j.jenvman.2017.01.053>
- Kusimi, J. M. (2008). Assessing land use and land cover change in the Wassa West District of Ghana using remote sensing. *GeoJournal*, *71*(4), 249–259. <https://doi.org/10.1007/s10708-008-9172-6>
- Kuusaana, E. D., & Eledi, J. A. (2015). As the city grows, where do the farmers go? Understanding Peri-urbanization and food systems in Ghana - Evidence from the Tamale Metropolis. *Urban Forum*, *26*(4), 443–465. <https://doi.org/10.1007/s12132-015-9260-x>
- Lewis, S. L., Edwards, D. P., & Galbraith, D. (2015). of tropical forests. *Science*, *349*, 827–832.
- Li, Z., Liu, X., Niu, T., Kejia, D., Zhou, Q., Ma, T., & Gao, Y. (2015). Ecological restoration and its effects on a regional climate: The source region of the yellow river, China. *Environmental Science and Technology*, *49*(10), 5897–5904. <https://doi.org/10.1021/es505985q>
- Li, Z., Wang, Z., Liu, X., Fath, B. D., Liu, X., Xu, Y., ... Kroeze, C. (2019). Causal relationship in the interaction between land cover change and underlying surface climate in the grassland ecosystems in China. *Science of the Total Environment*, *647*, 1080–1087. <https://doi.org/10.1016/j.scitotenv.2018.07.401>
- Mu, Q., Zhao, M., & Running, S. W. (2013). MODIS Global Terrestrial Evapotranspiration (ET) Product (NASA MOD16A2/A3) Collection 5. *Numerical Terradynamic Simulation Group*.
- Nang, B. (2016). Anthropogenic and Institutional Determinants of Forest Resource Degradation in the Savanna Ecological Zone of Northern Ghana. *Research Journal of Environmental and Earth*

Sciences, 8(4), 44–55. <https://doi.org/10.19026/rjees.8.3065>

Schoneveld, G. C., & German, L. (2014). Translating Legal Rights into Tenure Security: Lessons from the New Commercial Pressures on Land in Ghana. *Journal of Development Studies*, 50(2), 187–203. <https://doi.org/10.1080/00220388.2013.858129>

Schueler, V., Kuemmerle, T., & Schröder, H. (2011). Impacts of surface gold mining on land use systems in Western Ghana. *Ambio*, 40(5), 528–539. <https://doi.org/10.1007/s13280-011-0141-9>

Tutu Benefoh, D., Villamor, G. B., van Noordwijk, M., Borgemeister, C., Asante, W. A., & Asubonteng, K. O. (2018). Assessing land-use typologies and change intensities in a structurally complex Ghanaian cocoa landscape. *Applied Geography*, 99(October 2017), 109–119. <https://doi.org/10.1016/j.apgeog.2018.07.027>